

https://doi.org/10.1070/QEL17049

Laser photoionisation selectivity of ^{177}Lu radionuclide for medical applications

I.V. Ageeva, A.B. D'yachkov, A.A. Gorkunov, A.V. Labozin, S.M. Mironov, V.Ya. Panchenko, V.A. Firsov, G.O. Tsvetkov, E.G. Tsvetkova

Abstract. **We consider the selectivity obtained by laser photoionisation of the ^{177}Lu radioisotope according to the three-stage $5d\,6s^2\ ^2D_{3/2}-5d\,6s\,6p\ ^4F^o_{5/2}-5d\,6s7s\ ^4D_{3/2}-(53375\ cm^{-1})^o_{1/2}$ scheme from the viewpoint of the task of isolating the radionuclide for medical use. The selectivity attained through various photoionisation channels and the impact of multiphoton processes and the laser radiation spectrum on the photoionisation selectivity are investigated.**

Keywords: *laser photoionisation, ^{177}Lu radionuclide, three-stage scheme.*

1. 1. Introduction

The paper is dedicated to the development of a laser photoionisation method for producing the ^{177}Lu radionuclide for medical use. The decay of ^{177}Lu (half-life of 6.7 days) releases beta radiation with an energy of ~500 keV and an effective radius of action in tissues less than 2 mm, which is considered to be the most suitable for the treatment of small tumours and metastases, with minimal impact on healthy organs and tissues. Concomitant soft gamma radiation with energy of 113 and 208 keV allows diagnostics (visualisation), dosimetry analysis, and treatment process optimisation in each case, implementing the principles of personalised medicine.

Currently, there are two main methods for producing this radioisotope, which are based on the irradiation of an isotope-enriched substance by a neutron flux in an atomic reactor. The first method uses a high neutron capture cross section (~2065 barn) by the ^{176}Lu nucleus (natural concentration of 2.6%). In an intense neutron flux (~2×10^{15} cm^{-2} s^{-1}), ^{177}Lu can be isolated at a concentration of ~60% by using highly enriched ^{176}Lu [1]. In moderate neutron fluxes (~10^{14} cm^{-2} s^{-1}), the ^{177}Lu concentration reaches 20% [2]. The disadvantage of this method is that the product contains a metastable ^{177m}Lu isomer with a half-life $T_{1/2}$ = 160 days, which complicates the storage of radioactive waste generated during the treatment of patients [3]. When ^{177}Lu is obtained by the second method, a target of highly enriched ^{176}Yb is used (natural concentration of 12.6%), which, upon capture of neutron, transforms into the ^{177}Yb ($T_{1/2}$ = 1.9 hours) with further decomposition and the formation of ^{177}Lu. Separation of ^{177}Lu from the ytterbium carrier is performed by chemical methods. The concentration of the radionuclide emitted by this method reaches a theoretical limit of ~100% [4]. The additional advantage of this method is the practical absence of ^{177m}Lu in the final product. However, the neutron capture cross section of the ^{176}Yb nucleus is 2.5 barn, which requires the use of large neutron fluxes – more than 10^{14} cm^{-2} s^{-1}. In addition, the efficiency of using the enriched ^{176}Yb is extremely low (~10^{-4}), which significantly increases the product cost.

When using a laser method of ^{177}Lu extraction, a target of natural metallic lutetium is irradiated by neutrons, resulting in a mixture of ^{175}Lu (97.4%), ^{176}Lu (2.6%), ^{177}Lu, and ^{177m}Lu isotopes. The concentration of ^{177}Lu, depending on the neutron flux intensity and duration of irradiation, can vary within 0.001%–1%, and the radionuclide can be extracted from the irradiated target by laser selective photoionisation. The essence of the laser method is that the irradiated metal target evaporates in vacuum at a temperature of 1700 °C, and a flow of target atoms passes through a zone filled with laser radiation, in which selective photoionisation occurs. The ^{177}Lu$^+$ photoions are extracted by an electric field and fed to the product collector, while the atoms of other isotopes, remaining neutral, continue their motion along a straight path to the dump collector. A three-stage optical scheme of lutetium photoionisation using dye lasers (DLs) pumped by copper vapour lasers was proposed in [5]. The hyperfine structure of the first radioisotope transition was studied in [6], in which selective ^{177}Lu photoionisation was first implemented and a selectivity of ~10^5 was obtained. It was shown experimentally in [7] that the proposed scheme makes it possible to attain high degrees of radionuclide extraction due to photoionisation. The structure of the second and third transitions in ^{177}Lu was studied in detail in [8].

In this paper, we investigate the selectivity of ^{177}Lu laser photoionisation for further medical application of the radioisotope obtained. It should be noted that until today there have been no clear requirements for the fraction of ^{177}Lu radioactive atoms in lutetium used in medicine. The fact is that ^{177}Lu is used in many medical techniques, most of them being under development. The basis of these techniques is the so-called targeted therapy which employs the means of targeted delivery of medicinal products. In this case, the medici-

I.V. Ageeva, E.G. Tsvetkova National Research Centre 'Kurchatov Institute', pl. Akad. Kurchatova 1, 123182 Moscow, Russia; I.M. Sechenov First Moscow State Medical University of the Ministry of Healthcare of the Russian Federation (Sechenov University), ul. Trubetskaya 8, stroenie 2, 119991 Moscow, Russia; **A.B. D'yachkov, A.A. Gorkunov, A.V. Labozin, S.M. Mironov, V.Ya. Panchenko, V.A. Firsov, G.O. Tsvetkov** National Research Centre 'Kurchatov Institute', pl. Akad. Kurchatova 1, 123182 Moscow, Russia; e-mail: Tsvetkov_GO@nrcki.ru, glebtsvetkov@mail.ru

Received 23 April 2019
Kvantovaya Elektronika **49** (9) 832–838 (2019)
Translated by M.A. Monastyrskiy

nal drug is a very large molecule with a molecular weight of more than 100 kDa. The molecule consists of a vector part that provides specificity to certain structural elements of affected tissues, and a chelating part designated to reliably retain radionuclide atoms. Monoclonal antibodies (radioimmune therapy) or receptor-specific proteins (peptide receptor radioimmune therapy) are used as a vector. Owing to the presence of the vector part, when introducing the medicinal drug into the patient's bloodstream, the drug accumulation is observed mainly in pathological tissues, whose cells, to a greater extent than normal tissues, express the antigen on their surface. Radiopharmaceutical accumulation can be monitored by detecting the ^{177}Lu soft gamma radiation by means of scintigraphy or resonance gamma tomography.

The most common chelating agent is 1,4,7,10-tetraazocyclododecyl-1,4,7,10-tetraacetic acid (DOTA). The structure of this molecule is a square antiprism, at the base of which there is a square, formed by four nitrogen atoms occupying places Nos 1, 4, 7, and 10 in a cycle of 12 vertices. The remaining vertices of the cycle are occupied by carbon atoms which are part of the CH_2 groups. The second base of the antiprism consists of a square, at the vertices of which oxygen atoms being part of the CH_2COOH acetic acid are located. Above the oxygen base, a water molecule is located. In the process of chelation, one lutetium atom forms 7–9 coordination bonds with nitrogen and oxygen atoms and turns out located inside the structural framework of the molecule.

One of the most important parameters is the average number of chelating agents attached to a single vector. An increase in the number of chelators enables one to increase the specific activity of the drug or, while maintaining the specific activity, to reduce the requirements for the specific activity of the radionuclide used for radioactive labelling. For example, in work [9] it was shown that an increase in the number of DOTA agents to four in compound with a Rituximab monoclonal antibody does not affect immunoreactivity, i.e., the ability of the latter to selectively bind to antigens expressed on the surface of tumour cells. On the other hand, increasing the number of DOTA agents to eight leads to a 50% decrease in Rituximab immunoreactivity. Thus, in each individual case, it seems necessary to optimise the number of chelating agents attached to a particular vector part.

In the vast majority of existing and developing techniques, the average number of chelators per vector is measured

Table 1. Medical techniques employing ^{177}Lu.

Antibody	Chelate compound	Number of chelators per antibody	Tumour (indications)	^{177}Lu concentration (%)	References
Anti-CD20 (Rituximab)	p-SCN-Bz-DOTA	4	Non-Hodgkin lymphomas	43.8	[9]
	DOTA-NHS-ester	4.9 ± 1.1		37.5	[10]
	p-NCS-benzyl-DOTA	6		31.9	[11]
Anti-L1-CAM	DOTA	2.5	Neuroblastomas	60.2	[11]
	DOTA	7	Renal cell carcinomas	28.0	[12]
		12		17.5	
		15	Ovarian and endometrium	14	
CC-49	DOTA-CC49	5.53	Gastrointestinal adenocarcinomas, ovarian carcinoma, breast endometrium	34.1	[13]
	MeO-DOTA-CC49	2.51		60.0	
	CHX-A″-DTPA	2.1		66.6	[14]
	C-DOTA	1.1		87.7	
	PA-DOTA	0.7		96.3	
Anti-Tenascin 81C6 mAb	ch81C6-NHS-DOTA	4.0	Glioma	43.8	[15]
	ch81C6-MeO-DOTA	4.5		40.1	
	C-DOTA	3.1		52.4	[16]
	MeO-DOTA	2.7		57.4	
cG250	^{177}Lu-cDTPA-cG250 ^{177}Lu-SCN-Bz-DTPA-cG250 ^{177}Lu-DOTA-cG250	1–3	Renal carcinoma	90–53.5	[17]
A33 (huA33)	CHX-AU-DTPA	4	Colorectal carcinoma	43.8	[18]
Hu3S193	^{177}Lu-CHX-A″-DTPA-hu3S193	3	Prostate cancer	53.5	[19]
J-591	DOTA	5	Prostate cancer	36.9	[20]
MOv18	^{177}Lu-DOTA-MOv18	2	Ovarian carcinoma	68.4	[21]
Pertuzumab	benzyl-CHX-A″-DTPA	2	Breast carcinoma	68.4	[22]
Trastuzumab (Herceptin)	DOTA-NHS	5.5–6	Breast carcinoma	34.2–31.9	[23]
	1B4M-DTPA	5		36.9	[24]

in various ways and is given in the literature, which allows us to estimate the required concentration of radioactive atoms in the employed radionuclide preparation.

In the presence of n chelators in the conjugate molecule, the fraction of p molecules in which all atoms are non-radioactive can be calculated by the formula

$$p = (1 - C_{177})^n, \quad (1)$$

where C_{177} is the concentration of ^{177}Lu in the radionuclide preparation. From here we obtain

$$C_{177} = 1 - p^{1/n}. \quad (2)$$

Table 1 provides information about a number of published medical techniques employing ^{177}Lu, with an indication of the average number of chelators per vector. Also shown are the values of C_{177} calculated by formula (2) with $p = 0.1$.

It follows from the data listed in Table 1 that the overwhelming majority of techniques can be implemented using the lutetium preparation with a concentration of ^{177}Lu, not exceeding 60%.

2. Experimental setup and photoionisation scheme

The studies were performed on a setup used for experiments on laser photoionisation spectroscopy in narrow collimated atomic beams, with the possibility of determining the isotopic composition of photoions. The setup consists of a vacuum chamber with a pump system, an evaporator, and an MS-7302 quadrupole mass spectrometer. The atomic beam formed by the evaporator enters the ion source of the mass spectrometer. For resonant excitation and ionisation of atoms, use is made of radiation from three pulsed single-mode DLs with a spectral line width of 100–120 MHz (FWHM), pumped by copper vapour lasers. Laser beams cross the atomic beam directly in the ionisation chamber of the ion source. The directions of atomic and laser beams, as well as the ion-optical axis of the mass spectrometer, are mutually orthogonal. Recording of ions in the mass spectrometer is performed by a secondary electron multiplier. Precision wavelength meters are used to control the DL generation wavelength. The setup control and data recording are carried out on-line. The software implemented in LabView environment (National Instruments) performs the necessary actions: receives data from wavelength meters, signals from the secondary electron multiplier, and tunes or stabilises each DL according the lasing wavelength by changing the control voltage using the interface unit. Technical parameters and features of the experimental setup are described in detail in [6].

A sample of natural metallic lutetium was irradiated for two days in a dry channel of the IR-8 (Kurchatov Institute) research reactor in a neutron flux of 3×10^{13} cm^{-2} s^{-1}. At the time of the experiment (seven days after irradiation), the ^{177}Lu concentration measured by gamma spectroscopy constituted $(3.4\pm0.4)\times10^{-5}$.

The photoionisation scheme used in the experiment is shown in Fig. 1. The ground state 5d 6s^2 ^{2}D$_{3/2}$ (energy $E = 0$) is split into four sublevels ($F = 2, 3, 4, 5$). At an evaporation temperature of 1700 °C, the equilibrium population of the lower level is $\sim$0.7, and the population of each sublevel is proportional to its statistical weight $2F + 1$. In accordance with the rules for selecting dipole transitions, a transition with $\Delta F = 0, \pm1$ is possible from each state. Thus, there exist a large number of photoionisation channels with a certain set of sublevels, which vary both in the transition frequencies and in the

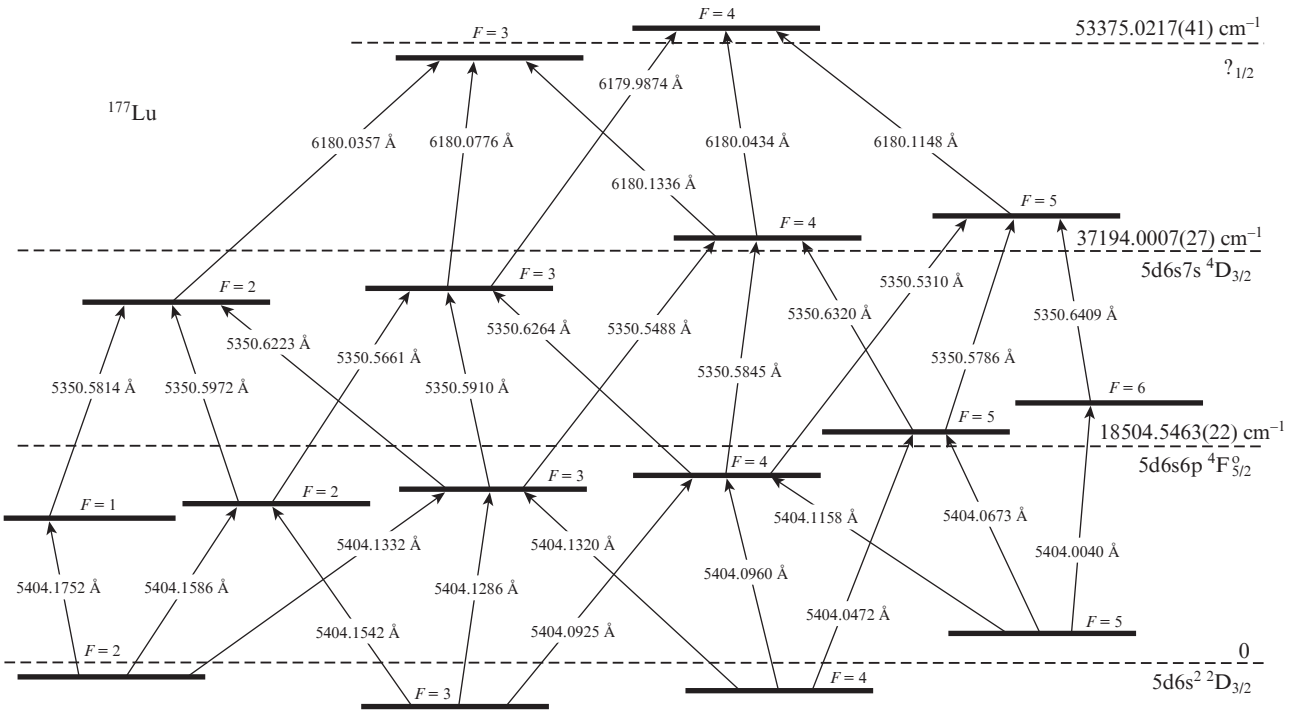

Figure 1. Photoionisation scheme of ^{177}Lu [8].

fraction of ^{177}Lu atoms involved in the photoionisation process.

3. Selective photoionisation of ^{177}Lu

In the case of the laser isotope separation method, selectivity is defined as a ratio of the photoionisation probabilities of the target and non-target isotopes. Obviously, for the efficient isolation of isotope with an initial concentration of 10^{-4}–10^{-5}, the ionisation process selectivity should exceed 10^5. Experiments on laser photoionisation of the ^{150}Nd and ^{63}Ni isotopes [25, 26], as well as the results of laser isolation of the ^{176}Yb and ^{168}Yb isotopes [27] show that the attainment of a selectivity of $\sim 10^5$ requires the target isotope excitation to be selective at all stages of the photoionisation scheme (isotopic shift at all transitions should exceed 0.5–1 GHz).

In order to attain maximum selectivity of ^{177}Lu laser photoionisation, in this work we have determined and studied the ionisation channels with the highest isotopic shifts at all excitation stages, derived an assessment of the effect on the selectivity of nonresonant two-photon processes, and identified the permissible level of amplified spontaneous emission in DL beams.

3.1. Selection of ionisation channels

Since the lutetium isotopes ^{175}Lu, ^{176}Lu, ^{177}Lu, and ^{177m}Lu have a nonzero nuclear spin, the excitation selectivity, along with the values of isotopic shifts, is determined by the hyperfine structure of the transitions. Due to the hyperfine splitting of the levels of the three-stage scheme $5d\,6s^2\ ^2D_{3/2}$– $5d\,6s\,6p\ ^4F^o_{5/2}$–$5d\,6s\,7s\ ^4D_{3/2}$–$(53375\ см^{-1})^o_{1/2}$, the ionisation of any isotope can pass through 44 natural frequency excitation/ionisation channels. Obviously, there is a probability of overlapping transition frequencies for the target and non-target isotopes at different levels of excitation, which inevitably leads to a decrease in selectivity for a given ionisation channel. The overlapping of several lines of the ^{177}Lu target isotope on the ^{175}Lu and ^{176}Lu lines of the first stage was clearly demonstrated in [6]. Analysis of the hyperfine structure of transitions at all stages of the scheme made it possible to determine the most selective ^{177}Lu excitation channels, which are presented in Table 2. For each scheme, Table 2 indicates the nearest excitation channels of the ^{175}Lu, ^{176}Lu, ^{177m}Lu isotopes and frequency distances to the ^{177}Lu transitions at all ionisation stages. For ^{177m}Lu, a calculated estimate for the first stage is given according to [28].

Five ionisation channels with similar frequency shifts turned out the most selective with respect to ^{175}Lu (the content was 97.4%). For each of these channels, the closest was a similar ^{175}Lu ionisation channel, while the distances to the ^{175}Lu lines at the stages constituted in average 1.2, –0.6 and 0.2 GHz. This is explained by the similarity of the ^{175}Lu and ^{177}Lu hyperfine structures with the same nuclear spins (I = 7/2) and close values of magnetic dipole moments: μ^{177} = 2.2384(14)μ_N [29], μ^{175} = 2.2323(11)μ_N [30]. Obviously, the ionisation channels 3–4–3–4 and 4–5–4–3 (Table 2) are less selective due to the presence at the first stage of a close line of ^{175}Lu that is excited to the same sublevel as ^{177}Lu from another lower sublevel. The frequency distance to the nearest ^{175}Lu and ^{176}Lu lines at the transitions $2\to2$, $3\to2$, $4\to4$, $5\to4$ does not exceed 100 MHz and, therefore, the corresponding ionisation channels were not considered.

Table 2. Selective channels of ^{177}Lu photoionisation (by hyperfine structure components).

^{177}Lu, $F\to F$ photoionisation channel	Excitation channel and frequency shift /MHz		
	^{175}Lu	^{176}Lu	^{177m}Lu
5–6–5–4	5–6–5–4 1192; –587; 212	7.5–8.5–7.5–6.5 –904; –1948; –3550	13–14 575
5–5–5–4	5–5–5–4 1192; –618; 212	6.5–7.5–7.5–6.5 257; –1446; –3550	12–12 –31
4–5–4–3	5–5–4–3 –873; –618; 267	8.5–8.5–7.5–6.5 1058; –1980; –2074	13–13 –10
4–3–4–3	4–3–4–3 1222; –618; 267	7.5–6.5–7.5–6.5 1048; 493; –2074	10–10 –226
3–4–3–4	4–4–3–4 863; –587; 212	8.5–7.5–6.5–7.5 –401; –2316; 1587	12–12 –514
2–3–4–3	2–3–4–3 1202; –618; 267	7.5–6.5–7.5–6.5 1171; 493; –2074	10–10 –103
2–1–2–3	2–1–2–3 1233; –629; 244	5.5–5.5–6.5–6.5 1685; 2232; –3935	10–9 1664

The ^{176}Lu hyperfine structure (2.6%) differs from that of the ^{177}Lu target isotope (I = 7, μ^{176} = 3.169(5)μ_N [29]). As a result, with a relatively small frequency shift at the first transition (0.3–0.4 GHz), there are ionisation channels with shifts of 2–3 GHz at the subsequent stages (5–5–5–4 and 3–4–3–4, Table 2).

Relative to the ^{177m}Lu isomer, the channels 5–6–5–4, 3–4–3–4, and 2–1–2–3 are selective at the first stage. Other channels (Table 2) may also be selective. The fact is that the isomer content is extremely small and, therefore, the requirements for the selectivity of ^{177}Lu photoionisation are reduced – it can be several orders of magnitude less. Due to the differences in hyperfine isotope structures (I = 23/2, μ^{177m} = 2.337(13)μ_N [31]), there is a possibility that the transitions of the second and/or third stages would turn out selective.

Particular attention should be paid to the 4–3–4–3 ionisation channel, where the line $2\to3$ is located next to the line $4\to3$ of the first stage at a distance of 120 MHz. When adjusting the lasing frequency, for example, between these lines, in the regime of transition saturation at a spectral width of generation line of 100–150 MHz (FWHM), atoms can be simultaneously transferred to the sublevel with F = 3 from the two lower sublevels with F = 4 and 2. Relative populations of these sublevels are 0.28 and 0.16; therefore, the proportion of atoms involved in the photoionisation process can be increased up to 44%.

Laser photoionisation of ^{177}Lu was performed by the most selective ionisation channels from Table 2. The initial concen-

Table 3. Selective photoionisation of ^{177}Lu via different ionisation channels.

^{177}Lu, $F\to F$ photoionisation channel	Relative population of lower sublevel	Concentration of ^{177}Lu photoions	Selectivity $S^{**}/10^5$
5–6–5–4	0.34	0.80(2)	1.2(2)
5–5–5–4	0.34	0.90(1)	2.7(3)
4–3–4–3	0.28	0.92(1)	3.4(5)
2–3–4–3	0.16	0.88(2)	2.2(4)
(4+2)–3*–4–3	0.16 + 0.28	0.93(1)	4.0(6)

* First-stage laser radiation frequency was tuned between the $4\to3$ and $2\to3$ transitions.

** $S = C_p(1 - C_f)/[(1 - C_p)C_f]$, where C_p – is the content of ^{177}Lu and C_f – is the initial concentration of ^{177}Lu.

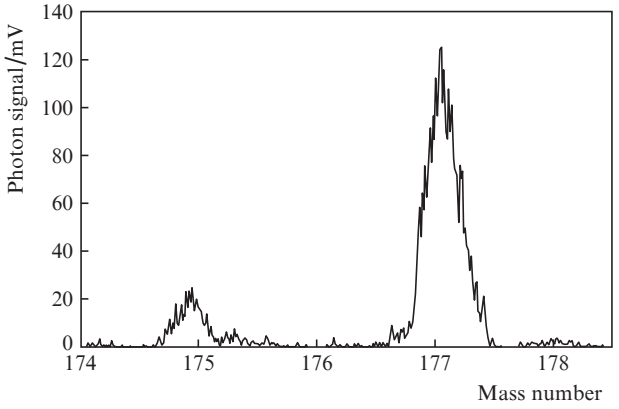

Figure 2. Mass spectrum of photoions in selective ionisation of ^{177}Lu via the 5–6–5–4 channel.

tration of the target isotope in the evaporated sample was $(3.4\pm0.4)\times10^{-5}$. The average laser power densities were close to the transition saturation levels [6] and amounted to 3, 3, and 2000 mW cm^{-2} for stages. Laser pulses for the second and third stages were delayed relative to the first-stage pulse for a time equal to the laser pulse duration (~20 ns). The experimental results are summarised in Table 3. For all ionisation channels, the concentration of ^{176}Lu photoions did not exceed 0.01–0.02.

The mass spectrum of photoions in selective ionisation of ^{177}Lu through the channel 5–6–5–4 is shown in Fig. 2.

3.2. Effect on selectivity of nonresonant two-photon absorption

It was found in experiments that selectivity of photoionisation process increases considerably with the delay of laser pulses for the second and third stages by a time equal to the laser pulse duration (~20 ns). The effect of two-photon processes on selectivity lies in the fact that the probability of two-photon transition depends in a greater degree on the detuning from the upper level energy of the sum of quantum energies rather than on the detuning of individual transitions [32]. For example, from Table 2 it follows that, with fine tuning of the first ^{177}Lu transition 5→6 for the corresponding ^{175}Lu transition, the detuning is 1192 MHz. For the second transition 6→5, the detuning is –587 MHz. In the case of a stage-like resonance process, the transitions occur independently and the first transition selectivity attained due to the spectral contrast of laser radiation is multiplied by the similar selectivity of the second transition. On the contrary, in the case of two-photon processes, the probability of undesirable photoionisation of ^{175}Lu is largely determined by the detuning of the sum of quantum energies from the energy of the second excited state, which in this case constitutes 605 MHz. Thus, the superimposition of pulses in time opens up a possibility of two-photon transitions, which increases the probability of undesirable photoionisation of ^{175}Lu and reduces the final selectivity of the process.

An experimental study of the effect of two-photon processes on the selectivity of photoionisation was conducted for the 5–6–5–4 ionisation channel (Table 4). Using the formulas and selectivity values from Table 4, it is easy to obtain the following relations: $S_1S_2/S_{12} = 2.1$ and $S_2S_3/S_{23} = 4.6$. This

Table 4. Effect of multiphoton processes on the selectivity of ^{177}Lu photoionisation via the 5–6–5–4 channel.

Temporal configuration of pulses on stages	Selectivity formula	Concentration of ^{177}Lu photoions (%)	Selectivity/10^5
$\lambda_1\rightarrow\lambda_2\rightarrow\lambda_3$	$S = S_1S_2S_3$	95(1)	5.5(4)
$\{\lambda_1,\lambda_2\}\rightarrow\lambda_3$	$S = S_{12}S_3$	90(1)	2.6(3)
$\lambda_1\rightarrow\{\lambda_2,\lambda_3\}$	$S = S_1S_{23}$	80(2)	1.2(2)
$\{\lambda_1,\lambda_2,\lambda_3\}$	$S = S_{123}$	67(1)	0.6(1)

Notes: S_i is the selectivity of a resonant single-stage process; S_{ij} is the process selectivity when laser pulses are superimposed in time for the ith and jth stage with a possibility of two-photon transitions; arrows indicate the presence of a time delay (20 ns) between pulses for the corresponding stages; curly brackets indicate pulses that are superimposed in time.

means that the superimposition of pulses in time for the first and second stages leads to the selectivity decrease by a factor of 2.1, while the superimposition of pulses for the second and third steps reduces the selectivity by a factor of 4.6 compared to the resonant single-stage processes. Thus, the effect of two-photon processes manifests itself to the greatest extent for the second and third transitions. This can be explained by the fact that the detuning of the sum of quantum energies for the second and third stages (375 MHz) is much smaller than that for the first and second stages (605 MHz), while the natural width of the upper autoionisation level constitutes 730 MHz [8].

3.3. Amplified spontaneous emission from DLs

The deselecting effect of amplified spontaneous emission (ASE) is possible if the wavelengths of transitions to excited states from the ground or lower metastable atomic states fall at a certain stage in the ASE spectrum of the DL beam, with the corresponding involvement of non-target isotopes into the ionisation process.

Earlier experiments on laser photoionisation of ^{177}Lu according to the scheme $5d\,6s^2\ ^2D_{3/2}$ (E = 0) → $5d\,6s\,6p\ ^4F^o_{5/2}$ (18505 см$^{-1}$) → $5d\,6s\,7s\ ^4D_{3/2}$ (37194 см$^{-1}$) → (53375 см$^{-1}$)$^o_{1/2}$ have revealed a strong effect on the selectivity of the ASE process for the third stage of the photoionisation scheme (618 nm) [33]. Even though the DL's amplified spontaneous emission spectrum (600–620 nm, SR640 dye) did not contain the first-stage transition wavelength (540 nm), the spectrum contained radiation with a wavelength of 606 nm, transferring atoms to the first excited state from the lower metastable level (E = 1994 cm^{-1}, population ~0.2): $5d\,6s^2\ ^2D_{5/2} \rightarrow 5d\,6s\,6p\ ^4F^o_{5/2}$. The spectral filtering method proposed in [33] (placing a mirror between the master oscillator and DL amplifier, which has a high transmittance at the lasing wavelength and high reflection in the region of the dye's luminescence maximum) made it possible to reduce the ASE level by 25 times (to 0.6%) and, as a consequence, to attain a selectivity of 10^5. However, the background substrate was responsible for about half of the photoions of the ^{175}Lu non-target isotope. To further reduce the ASE level in the DL for the third stage, a double pass through the filter-mirror was used, which made it possible to decrease the ASE level to 0.06% without significant loss of output power of this DL. Table 5 shows the results of ^{177}Lu photoionisation experiments performed for three conditions differing in the ASE levels. These experiments were conducted

Table 5. Effect of amplified spontaneous emission of the DL for the third stage on photoionisation selectivity of ^{177}Lu.

Number of passes though a filter-mirror	ASE level* (%)	Concentration of ^{177}Lu photoions (%)	Selectivity/10^4
–	15	9(2)	0.3(1)
1	0.6	67(2)	6(1)
2	0.06	80(2)	12(2)

*At an average output DL power (618 nm) of ~4 W.

for the 5–6–5–4 channel, with the laser pulses for the second and third stages superimposed and delayed by ~20 ns relative to the first-stage pulse.

In the two-pass case, in the absence of the beam for the first stage, the photoion signal of the ^{175}Lu non-target isotope was not observed; therefore, at the attained level of ~0.1%, the deselecting ASE effect was virtually absent.

4. Conclusions

Literature analysis shows that lutetium with a concentration of ^{177}Lu of about 60% can be used in the vast majority of modern medical techniques. The selectivity of ^{177}Lu photoionisation attained in the experiments corresponds to this value. Particular attention deserves the case when all laser pulses are superimposed in time and have intensities corresponding to the saturation of the transitions. Previously in work [7], under these conditions, the target isotope's photoionisation efficiency of 70% was attained for the 5–6–5–4 channel. In the present work, under the same conditions, the ^{177}Lu concentration of 67% was obtained for the 5–6–5–4 channel [$0.6(1)\times10^5$ selectivity). At the same time, there is a very significant reserve for increasing the initial concentration of ^{177}Lu by increasing the irradiation time and neutron flux intensity.

A number of photoionisation channels have been revealed, which are not inferior in selectivity and photoionisation efficiency to the 5–6–5–4 channel. These are primarily the combined (4 + 2)–3–4–3 and 5–5–5–4 channels which require more detailed study. The presence of selective channels performing photoionisation not only from the $F = 5$ sublevel, but also from the $F = 2$, 4 sublevels opens up the possibility of attaining, on an industrial installation, the ^{177}Lu extraction degree of about 50%, with simultaneous use of the photoionisation channels from the $F = 2$, 4, 5 sublevels. Multiphoton and, in particular, two-photon processes have a significant impact on the selectivity of photoionisation. The maximum selectivity of $5.5(4)\times10^5$ has been attained with the successive action of pulses for the first, second, and third stages, when multiphoton processes are impossible. Selectivity decreases with the superimposition of pulses in time, and to the greatest extent – due to two-photon processes at the second and third stages. Under these conditions, a sophisticated optimisation of intensities for all three photoionisation stages is required.

In the third-stage laser, a regime is implemented in which the ASE does not virtually affect the selectivity of ^{177}Lu photoionisation.

Acknowledgements. The authors are grateful to S.S. Arzumanov, Yu.N. Panin, Yu.V. Vyazovetskii, and D.Yu. Chuvilin for their assistance in the preparation of the ^{177}Lu sample.

The study was supported by a grant of the Russian Science Foundation (Project No. 17-13-01180).

References

1. Toporov Y.G., Tarasov V.A., Andreyev O.I., Zotov E.A., Gavrilov V.D., Kupriyanov A.L., Kuznetsov R.A. *Proc. IAEA Headquarters* (Vienna, Austria, 2006).
2. Pillai M., Chakraborty S., Das T., Venkatesh M., Ramamoorthy N. *Appl. Radiat. Isot.*, **59**, 109 (2003).
3. Henkelmann R., Hey A., Buck O. *Physics for Health in Europe* (CERN, 2010).
4. Banerjee S., Pillai M.R.A., Knapp F.F. *Chem. Rev.*, **115**, 2934 (2015).
5. D'yachkov A.B., Kovalevich S.K., Labozin A.V., Labozin V.P., Mironov S.M., Panchenko V.Ya., Firsov V.A., Tsvetkov G.O., Shatalova G.G. *Quantum Electron.*, **42**, 953 (2012) [*Kvantovaya Elektron.*, **42**, 953 (2012)].
6. D'yachkov A.B., Firsov V.A., Gorkunov A.A., Labozin A.V., Mironov S.M., Panchenko V.Y., Semenov A.N., Shatalova G.G., Tsvetkov G.O. *Appl. Phys. B*, **121**, 425 (2015).
7. D'yachkov A.B., Gorkunov A.A., Labozin A.V., Mironov S.M., Panchenko V.Ya., Firsov V.A., Tsvetkov G.O. *Quantum Electron.*, **48**, 1043 (2018) [*Kvantovaya Elektron.*, **48**, 1043 (2018)].
8. D'yachkov A.B., Gorkunov A.A., Labozin A.V., Mironov S.M., Tsvetkov G.O., Panchenko V.Y., Firsov V.A. *Opt. Spectrosc.*, **125**, 839 (2018).
9. Forrer F., Chen J.F.M., Powell P., Lohri A., Müller-Brand J., Moldenhauer G., Maecke H.R. *Eur. J. Nucl. Med. Mol. Imaging*, **36**, 1443 (2009).
10. Massicano A.V.F., Pujatti P.B., Alcarde L.F., Suzuki M.F., Spencer P.J., Araújo E.B. *Curr. Radiopharm.*, **9**, 54 (2016).
11. Guleria M., Das T., Kumar C., Rohit S., Amirdhanayagam J., Sarm H.D., Dash A. *Anticancer. Agents Med. Chem.*, **18**, 146 (2018).
12. Knogler K., Grünberg J., Novak-Hofer I., Zimmermann K., Schubiger P.A. *Nucl. Med. Biol.*, **33**, 883 (2006).
13. Mohsin H., Jia F., Sivaguru G., Hudson M., Shelton T., Hoffman T., Cutler C., Ketring A., Athey P., Simón J., Frank R., Jurisson S., Lewis M. *Bioconjugate Chem.*, **17**, 485 (2006).
14. Milenic D.E., Garmestani K., Chappell L.L., Dadachova E., Yordanov A., Ma D., Schlom J., Brechbiel M.W. *Nucl. Med. Biol.*, **29**, 431 (2002).
15. Yordanov A.T., Hens M., Pegram C., Bigner D.D., Zalutsky M.R. *Nucl. Med. Biol.*, **34**, 173 (2007).
16. Hens M., Vaidyanathan G., Zhao X.-G., Bigner D.D., Zalutsky M.R. *Nucl. Med. Biol.*, **37**, 741 (2010).
17. Brouwers A.H., Eerd-Vismale J., Frielink C., Oosterwijk E., Oyen W.J.G., Corstens F.H.M., Boerman O.C. *J. Nucl. Med.*, **45** (2), 327 (2004).
18. Almqvist Y., Steffen A.-C., Tolmachev V., Divgi C.R., Sundin A. *Nucl. Med. Biol.*, **33**, 991 (2006).
19. Burvenich I., Lee F., O'Keefe G., Makris D., Cao D., Gong S., Rigopoulos A., Allan L., Brechbiel M., Liu Z., Ramsland P., Scott A. *Eur. J. Nucl. Med. Mol. Imaging Res.*, **6**, 26 (2016).
20. Vallabhajosula S., Nikolopoulou A., Jhanwar Y.S., Kaur G., Tagawa S.T., Nanus D.M., Bander N.H., Goldsmith S.J. *Curr. Radiopharm.*, **9**, 44 (2016).
21. Zacchetti A., Coliva A., Luison E., Seregni E., Bombardieri E., Giussani A., Figini M., Canevari S. *Nucl. Med. Biol.*, **36**, 759 (2009).
22. Persson M., Tolmachev V., Andersson K., Gedda L., Sandström M., Carlsson J. *Eur. J. Nucl. Med. Mol. Imaging*, **32**, 1457 (2005).
23. Rasaneh S., Rajabi H., Babaei M.H., Daha F.J. *Nucl. Med. Biol.*, **37**, 949 (2010).
24. D'Huyvetter M.V., Vincke C., Xavier C., Aerts A.I., Baatout S.D., Muyldermans S., Caveliers V., Devoogdt N., Lahoutte T. *Theranostics*, **4**, 708 (2014).
25. Babichev A.P., Grigoriev I.S., Grigoriev A.I., Dorovskii A.P., D'yachkov A.B., Kovalevich S.K., Kochetov V.A., Kuznetsov V.A., Labozin V.P., Matrakhov A.V., Mironov S.M., Nikulin S.A., Pesnya A.V., Timofeev N.I., Firsov V.A., Tsvetkov G.O., Shatalova G.G. *Quantum Electron.*, **35**, 879 (2005) [*Kvantovaya Elektron.*, **35**, 879 (2005)].
26. Tsvetkov G.O., D'yachkov A.B., Gorkunov A.A., Labozin A.V., Mironov S.M., Firsov V.A., Panchenko V.Ya. *Quantum Electron.*, **47**, 48 (2017) [*Kvantovaya Elektron.*, **47**, 48 (2017)].

27. Hyunmin P., Duck-Hee K., Yongho C., Sungmo N., Tak-Soo K., Jaemiri H., Yorigjoo R., Do-Young J., Cheol-Jung K. *J. Korean Phys. Soc*., **49**, 382 (2006).
28. Georg U., Borchers W., Keim M., Klein A., Lievens P., Neugart R., Neuroth M., Rao P.M., Schulz C. *Eur. Phys. J. A*, **3**, 225 (1998).
29. Petersen F.R., Shugart H.A. *Phys. Rev*., **126**, 252 (1962).
30. Brenner T., Büttgenbach S., Rupprecht W., Träber F. *Nucl. Phys. A*, **440**, 407 (1985).
31. König C., Hinfurtner B., Hagn E., Zech E., Eder R. *Phys. Rev. C*, **54**, 1027 (1996).
32. Baranov V.I. (Ed.) *Izotopy: svoystva, polucheniye, primeneniye* (Isotopes: Properties, Preparation, Applications) (Moscow: IzdAt, 2000).
33. D'yachkov A.B., Gorkunov A.A., Labozin A.V., Mironov S.M., Panchenko V.Ya., Firsov V.A., Tsvetkov G.O. *Quantum Electron.*, **46**, 574 (2016) [*Kvantovaya Elektron.*, **46**, 574 (2016)].